ORIGINAL ARTICLE

Surface-coated PVDF@TAPEG selective ultrafiltration membranes: an investigation on membranes' hydrophilicity, and antifouling characteristics for effective humic acid removal from wastewater

Leila Emadinezhad[1] · Bita Ayati[1]

Abstract
This research aimed to synthesize polyvinyl fluoride membranes and coat them with tannic acid (TA) nanoparticles and polyethylene glycol (PEG) additives so that the membrane's removal efficacy for humic acid (HA) pollutant from agricultural wastewater was investigated. Thus, six membranes with PEG:TA ratios of 0:0, 1:0, 0:1, 1:1, 4:1, and 1:4 were synthesized. Then, the membranes' characteristics were identified by FTIR-ATR, FESEM, and AFM analysis, and HA's particle size and zeta potential were also investigated. Based on optimizing effective parameters, the operating pressure of 1.5 bar and HA concentration of 80 ppm were selected as optimal values. The membrane with PEG:TA = 4:1, as the optimally modified membrane, had a pure water flux of 446.03 L/m^2.h, effluent flux of 72.43 L/m^2.h, and pollutant removal rate of 86.62% at pH = 7 after 60 min had passed. These values for the pristine membrane (PEG:TA = 0:0) were 265.64 L/m^2.h, 89.39 L/m^2.h, and 75.59%, respectively. The results showed that although the effluent flux was lower in the optimized modified membrane than in the pristine membrane, HA removal percentage was increased.

Keywords Wastewater treatment · Tannic acid coating · Polyvinylidene fluoride membrane · Hydrophilicity · Humic acid separation

Introduction

Humic acid (HA) with carbonyl, quinone, carboxyl, and hydroxyl functional groups in aromatic and organic ring frameworks, as one of the main components of organic substances soluble in natural waters, plays an influential role in improving soil fertility. However, its presence in the environment due to the formation of HA-metal complex ions leads to the displacement of the metal during diffusion in the soil (Nazri et al. 2021; Teow et al. 2017). Also, the conventional treatment of water contaminated with HA causes chlorine to interact with HA, producing a series of carcinogenic substances for humans. Therefore, it is necessary to remove HA before the chlorination process in wastewater treatment plants. Among several purification methods, including coagulation, electrocoagulation, flotation, oxidation, and membrane separation, membrane separation acts as an innovative technology to separate water from pollutants such as water/oil mixture, microorganisms, proteins, and humic substances (Algamdi et al. 2019; Kumar et al. 2016), and advantages such as compact design, easy operation, environmental friendliness, low energy consumption, no need for chemicals, selectivity, and operation at room temperature have increased this process in recent decades (He et al. 2020; Li et al. 2020; Tajik et al. 2024). However, fouling and, consequently, the high operating cost of the membrane is a subject that deserves discussion, and much research has been done on it. In fact, when the membrane surface is contaminated, not only does it reduce the flux, but it also increases the operation and maintenance costs (Kusworo et al. 2020; Tajik et al. 2023). Improving the characteristics of the membrane surface with a hydrophilic modifier (including polymer materials and inorganic nanoparticles) can significantly increase the antifouling performance of the membrane. Hydrophilic polymers such as polyvinyl alcohol, polyethylene glycol (PEG) derivatives, and zwitterionic

✉ Bita Ayati
   Ayati_bi@modares.ac.ir

   Leila Emadinezhad
   leila_emadinezhad@modares.ac.ir

1 Civil and Environmental Engineering Faculty, Tarbiat Modares University, P.O. Box 14115-397, Tehran, Iran

polymers have been used to increase membrane flux and reduce membrane fouling (Luo et al. 2020).

Polyvinyl fluoride (PVDF) membrane is known as the most widely used material among all existing polymeric membranes due to its outstanding properties. Nevertheless, PVDF polymer has a profoundly high fouling due to its inherent hydrophobic property. Therefore, various techniques have been reported to make the membrane surface hydrophilic, including mixing hydrophilic polymers or embedding inorganic nanoparticles, chemical modification, and stabilization of Polymers with hydrophilic moieties on the surface of membranes by coating (Makhetha and Moutloali 2018; Mat Nawi, et al. 2020; Yong et al. 2019).

Tannic acid (TA) is a low-cost, safe, and environmentally friendly polyphenol extracted from plants, such as tea leaves, oak wood, nettle, and Chinese gall. HA has anticarcinogenic, antimutagenic, and antioxidant properties with the ability to form macromolecules and metal ions and is widely used as a coagulant or polymeric coagulant for water and cationic dyes purification (Oulad et al. 2020; Xu et al. 2018). PEG is also a polyether with two functional groups, hydroxyl, and ether, which consists of repeated units of ethylene glycol [–(CH2CH2O)n] and is known as macrogol as well (D'souza and Shegokar 2016).

Much research has been done on PVDF polymeric membranes integrated with nanoparticles such as TA, graphene oxide (GO), and titanium dioxide (TiO_2) to remove various pollutants; some examples are mentioned below. In Zhao et al. (2019) studies, a PVDF membrane was coated with graphene oxide nanoparticles, which caused water permeability to be reduced from 1845 to 375 L/m^2.h, hydrophilicity, and negative surface area to be increased from -23.4 to -46.8. (The water contact angle was reduced from 73° to 56°.) In the research of Li et al. (2019), PVDF membrane coating was done by TA nanoparticles and polyvinyl pyrrolidone additive, which increased pure water flux ($> 16,000$ L/m^2.h), antifouling properties (FRR $> 99.5\%$ and emulsion rejection $> 99\%$) and hydrophilicity (54°) in the modified membrane. In the studies of Teow et al. (2020), the PVDF X500 TiO_2 membrane was presented for the removal of HA due to its smooth surface and reactive surface layer, good antifouling properties (FRR $= 78.24\%$), and initial water flux of 58.81 L/m^2.h. In the research of Jiang et al. (2021), with a single-step coating of HA/sodium periodate solution on the PVDF hydrophobic membrane, increased permeability flux (> 2400 LMH/bar) and oil removal $> 98\%$ for the hydrophilic and underwater super oleophobic modified PVDF membrane (water contact angle reduction from 121 to 32) was observed. Sun et al. (2021) coated dopamine on PVDF/TiO_2 membrane and observed high removal efficiency (99%) and permeate flux (1389 L/m^2.h) for oily wastewater. According to the research of Karimi et al. (2021), the synthesis of PVDF membrane and its modification by Cu_2S 0.2wt% to

remove reactive blue dye was obtained, which had a high water flux of 248.25 L/m^2.h and FRR $= 92.4\%$. Yan et al. (2022) coated the hydrogel on the PVDF membrane surface, which reduced the oil pollutant fouling on the membrane surface. Also, pure water flux increased by 214%, permeability increased by 127%, and oil recovery was observed by 99.6% (Yan et al. 2022). Recently, Ren et al. (2022), by surface modification of PVDF membrane with propyl sulfated chitosan, witnessed high hydrophilicity (39°) and antifouling properties (FRR $= 90.4\%$) after two cycles. In the studies of Abdulazeez et al. (2023), a PVDF membrane was incorporated with iron in order to remove oil. It indeed increased the pure water permeance from 59.9 L/m^2.h in the pristine membrane to 300.5 L/m^2.h, and oil rejection was more than 99% (Abdulazeez et al. 2023).

In this research, the surface modification of the PVDF pristine membrane was done by coating TA nanoparticles and PEG additives to remove HA. TA nanoparticles and PEG additives are both environmentally friendly and nontoxic, able to form hydrogen bonds. In this vein, the –OH present in TA nanoparticles communicate with the –O– present in PEG additives and form a hydrogen bond, which, by coating the membrane surface, improves the antifouling properties of the membrane, hydrophilicity, and permeability flux of pure water. Investigated parameters in the test include operating pressure (0.5, 1, 1.5, 1.8, and 2 bar), pollutant concentration (30, 50, 80, and 100 ppm), PEG: TA ratio (0:0, 1:0, 0:1, 4:1, and 1:4), and pH (5, 7, and 9) were optimized. Also, the separation performance and removal efficiency, membrane properties, morphology, roughness, hydrophilicity, and membrane antifouling properties were investigated in detail.

Experimental

Materials

HA was purchased from Sigma-Aldrich to prepare synthetic wastewater. PVDF polymer and dimethylformamide (DMF) solvent for membrane synthesis and TA nanoparticles, PEG 4000, DMAc solvent, and ethanol for membrane surface modification were obtained from Merck. HCl and NaOH, obtained from Merck, were used for pH adjustment. Deionized water was used in all stages of the research.

Synthesis of PVDF polymeric membrane

This part was presented in SI, Sect. "Introduction". Part 1.

PVDF UF membrane modification

This part was presented in SI, Sect. "Introduction". Part 2.

Membrane characterization

Fourier transform infrared spectroscopy (FTIR-ATR) (PerkinElmer Frontier model) was performed to identify the functional groups on the surface of the membranes. Membrane morphology and roughness were respectively identified by scanning electron microscope TESCAN model manufactured by Mira 3-XMU company and atomic force microscope manufactured by NT-MDT company and model TS-150. EDS spectroscopic analysis was used by scanning electron microscope TESCAN model manufactured by Mira 3-XMU company to observe the elements on the surface of the membrane. The water contact angle test (manufactured by CAG-20 company, Jikan model) was performed to determine the hydrophilicity of the membrane surface. As a matter of fact, for its measurement, the membrane was placed on a smooth surface. Water drops with a volume of approximately ten microliters was released on the membrane's surface, and photos were taken after reaching the equilibrium state. For each sample, the average contact angle at different points was considered. A dynamic light scattering device manufactured by Horiba Jobin Jyovin company, the SZ-100z model, was used to measure the particle size and zeta potential of HA particles. The porosity and average diameter of membrane pores were obtained to identify the effect of additives and nanoparticles on membrane morphology and permeability.

To obtain the porosity of the membranes, the wet and dry weight of a specific area of each membrane after 24 h of staying in deionized water and oven at 60 °C, respectively, were measured and obtained according to Eq. (1) (Ni et al. 2021). Due to the small number of nanoparticles, the insignificant effect of its density was ignored in the calculation of the membrane density, and only the density of water was considered.

$$\varepsilon = \frac{m_1 - m_2}{Al\rho_w} \tag{1}$$

where m_1 and m_2 are, respectively, the wet and dry mass of the membrane (gr), A the effective surface of the membrane (cm^2), l the thickness of the membrane (cm), ρ_w the water density (gr/cm^3), and ε is the porosity of the membrane.

According to Eq. (2), Gorot Leford-Ferry equation, the average pore diameter was estimated (Sakarkar et al. 2020).

$$D_m = \sqrt{\frac{(2/9 - 1/75\varepsilon) \times 32\eta lQ}{\varepsilon A P}} \tag{2}$$

where η is the water viscosity ($8.9*10^{-4}$ Pa.s), Q is the water flow rate (m^3/s), P is the applied pressure (Pa), and D_m is the average diameter of the pore.

Preparation of synthetic wastewater and determination of effective parameters

First, 1 gr of HA pollutant ($C_9H_9NO_6$) was dried at 105 °C for 2 h to prepare synthetic wastewater. Then, it was dissolved in 100 ml of 0.1 M NaOH, made up to volume with deionized water, and placed on the stirrer for 4 h. Then, it was placed in an ultrasonic bath for better homogenization, and finally, pH = 7 was reached with 4 M HCl. From the 1000 ppm stock solution, the desired concentrations of synthetic HA solution were prepared by dissolving the stock solution in specific amounts of deionized water (Kumar et al. 2016).

In order to find the optimal mode, the performance of HA separation from wastewater by the pristine and modified membranes was checked using the OFAT method with three repetitions. In this regard, at first, according to the permeate flux and pollutant removal percentage, the optimal initial pressure and concentration were respectively obtained for the M_0 membrane. Based on that, these parameters were measured for all membranes. Finally, the optimum pH for the final selected membrane was investigated. Table 1 shows the parameters examined in this research and their ranges. The range of parameters was selected based on the references of Singh and Purkait (2016); Shi et al. (2018).

Filtration test

The filtration test was carried out in the dead-end laboratory pilot, according to Fig. S1, with an effective separation area of 11.34 cm^2 and an effective volume of 250 ccs. The required operating pressure was applied by a nitrogen capsule.

The mass of pure water and HA was measured to obtain the membrane flux. The filtration test was continued until the flux reached at least 50% of the initial flux. The total duration of the test was 135 min, in which pure water was passed in the first 30 min and the last 15 min. The output mass of HA was measured every 3 min in the first 15 min and then every 15 min until it reached a stable value in about 90 min. To ensure the accuracy of the data, the information on each membrane was obtained after three

Table 1 Investigated parameters

Parameter	Range
Pollutant Concentration (ppm)	30, 50, 80, 100
PEG: TA (w%)	0:0 (M_0), 1:0 (M_1), 0:1 (M_2), 1:1 (M_3), 4:1 (M_4), 1:4 (M_5)
pH	5, 7, 9
Pressure (bar)	0.5. 1, 1.5, 1.8, 2

tests, and the flux of the tests performed was calculated according to Eq. (3) (Mohd Yatim and Boon Seng 2019).

$$J = \frac{M}{t.A.\rho} \tag{3}$$

where M is the mass of wastewater (g), t is the duration of the solution penetration (h), A is the active area of the membrane (m^2), ρ is the density of water (g/L), and J is the flux of wastewater (L/h.m^2).

The pollutant removal rate in the samples was calculated using Eq. (4) (Xu et al. 2020).

$$R\% = \left(1 - \frac{C_p}{C_f}\right) \times 100 \tag{4}$$

where C_p and C_f are the HA concentration of the permeate and feed solutions, respectively, and R is the percentage of pollutant removal. (The absorbance of the solution was read by spectrophotometer at $\lambda_{max} = 254$ nm.)

Fouling and resistances measurements of membranes

The pure water flux was measured before and after the HA flux measurement to determine the antifouling ability of the membranes. FRR(%) is membrane recovery ratio, R_r (%) is reversible resistance, R_{ir} (%) is irreversible resistance, and R_t (%) is the total resistance of the membrane, which are obtained from relations (5), (6), (7), and (8) were respectively calculated. RFR(%) is also the sum of reversible and irreversible resistances (Khoo et al. 2022; Fan et al. 2021).

$$FRR(\%) = [\frac{J_{w2}}{J_{w1}}] \times 100 \tag{5}$$

$$R_r(\%) = [\frac{J_{w2} - J_p}{J_{w1}}] \times 100 \tag{6}$$

$$R_{ir}(\%) = [\frac{J_{w1} - J_{w2}}{J_{w1}}] \times 100 \tag{7}$$

$$R_t(\%) = \left[\frac{J_{w1} - J_p}{J_{w1}}\right] \times 100 = R_r + R_{ir} = RFR(\%) \tag{8}$$

In Eqs. (5–8), J_{w1} is the pure water flux in the first min of the test before the effluent filtration test, J_{w2} is the pure water flux in the final min of the test after the effluent filtration test, and J_p is the effluent flux.

Results and discussion

Membrane separation performance

This section examines the membrane that is most optimized in terms of pressure, pollutant concentration, PEG:TA ratios, and pH. Additionally, the investigation focused on water contact angle, membrane resistance abilities, and membrane porosity to further ensure the optimal membrane.
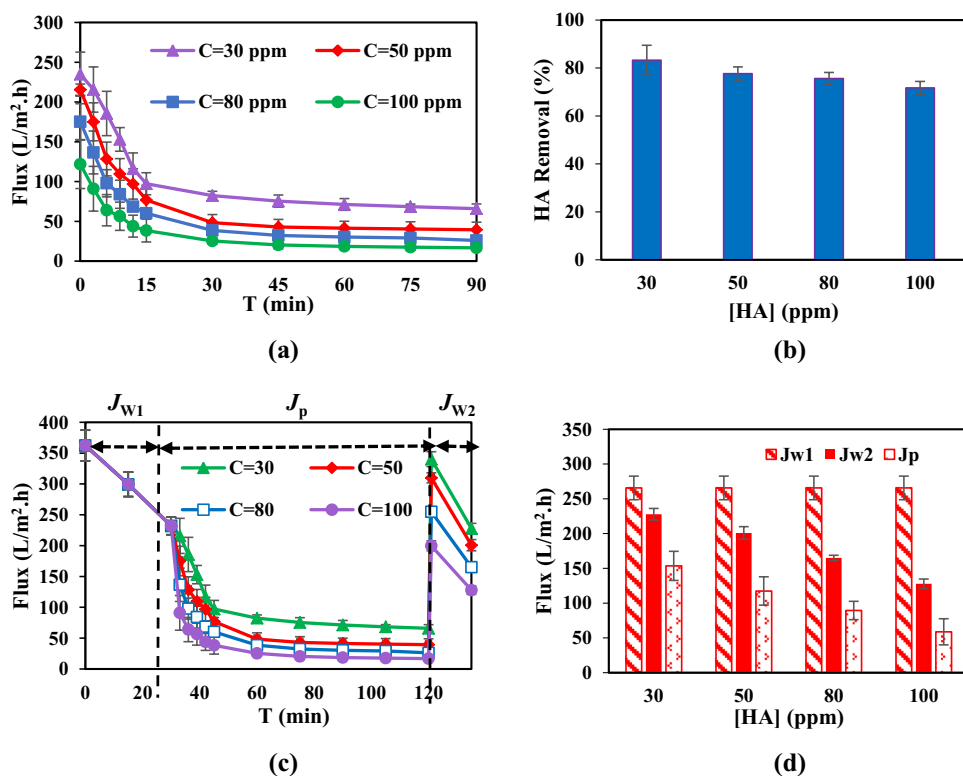
Operating pressure optimization

At first, the pure water flux was measured by passing the pure water before and after the wastewater passed through the membrane in order to investigate the operating pressure for the optimal M_0 membrane, the fouling, and membrane resistances (Fig. 1). As can be seen in Fig. 1 a, b, the amount of flux decreased slightly at pressures of 0.5 and 1 bar with the passage of time; however, with increasing pressure at pressures of 1.5, 1.8, and 2 times, the flux reduction has been significantly reduced in the first 15 min of the experiment. In fact, in the first min, the sharp and sudden decrease in the observed flux was due to membrane fouling and pollutant absorption on the clean surface of the membrane. Interestingly, among the particles that passed through the membrane pores, some of which had diameters almost equal to the membrane pores, were absorbed by the membrane wall, which resulted in a remarkable decrease in the flux in the first min. As it is evident, the increase in pressure is associated with the increase in flux. However, due to the higher pressure and also the rate of permeability, there is no room for pollutant absorption on the surface of the membrane, and a dense cake layer is formed on the surface of the membrane. As a result, the chance of membrane rejection and, subsequently, the removal percentage has decreased with increasing pressure. Alpatova et al. (2015) also mentioned similar results.

Figure 1 c, d, respectively, shows the total flux passing through the membrane in terms of time and the values of J_{w1}, J_{w2}, and J_p passing through the M_0 membrane at different pressures. According to these two forms, as expected, the pure water flux also increased with the increase of the applied pressure. This increase in flux was low at low pressures and more tangible at pressures higher than 1.5 bar, as in the research of Singh and Purkait (2016), similar results were presented. According to the results, the pressure of 1.5 bar, in which the increase in flux (117.38 L/m^2.h) and adequate rejection (77.63%) was observed, was chosen as the optimal pressure to continue the research.

Fig. 1 **a** Flux-time, **b** HA Removal (%), **c** General flux, **d** J_{w1}, J_{w2}, and J_p Flux changes passing through the M_0 membrane at different pressures during 90 min ((Nazri et al. 2021) = 50 ppm, pH = 7)
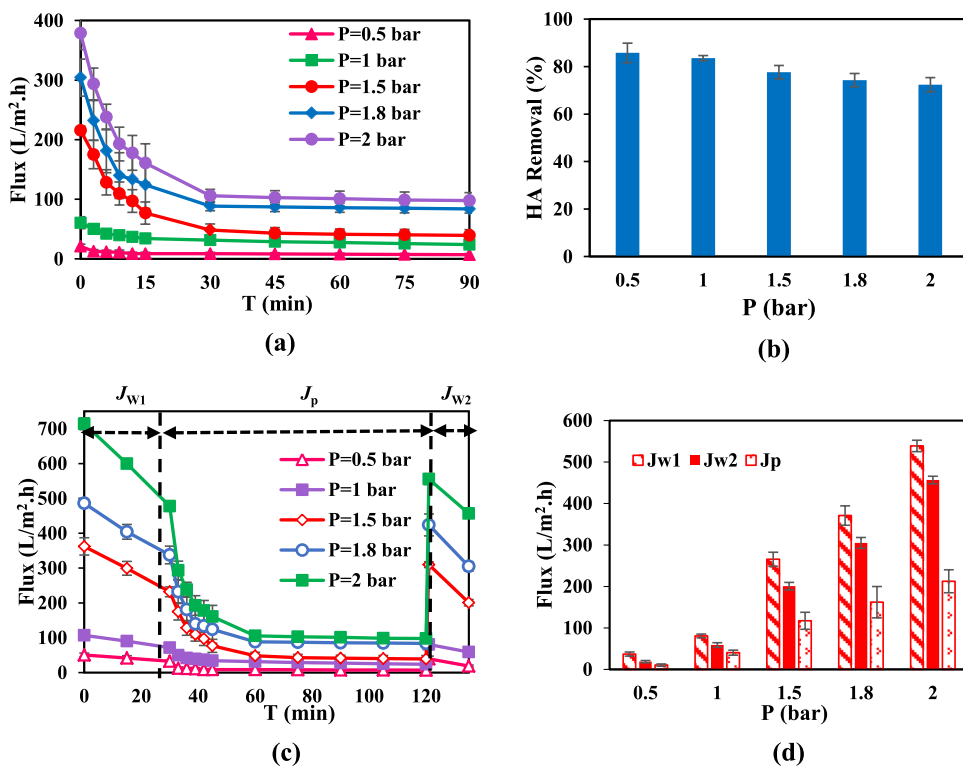
Fig. 2 **a** Flux-time, **b** HA Removal (%), **c** General flux, **d** J_{w1}, J_{w2}, and J_p Flux changes passing through the M_0 membrane at different concentrations of HA during 90 min ($P = 1.5$ bar, pH = 7)

Pollutant concentration optimization

After choosing the optimal operating pressure, the pollutant concentration was optimized for the M_0 membrane (Fig. 2). As can be seen in Fig. 2 a, b, in all concentrations, both the amount of flux and the percentage of removal have decreased over time, and also, the sudden drop of flux has happened in the first 15 min of pollutant passage. According to what was observed, increasing the concentration of HA means forming a thicker cake layer on the membrane, which reduces the flux. On the other hand, in high pollutant concentrations, the formation of the HA cake layer on the membrane surface was faster, which reduced the membrane absorption ability. It, in turn, led to the removal percentage decrease, which was also mentioned in the research of Singh and Purkait (2016). According to the investigation of the membrane flux and the pollutant removal percentage at different concentrations, the permeate flux and membrane rejection decreased slightly at higher pollutant concentrations.

Figure 2 c, d, respectively, shows the total flux passing through the membrane in terms of time and the values of J_{w1}, J_{w2}, and J_p passing through the M_0 membrane at different pollutant concentrations. As can be seen that with the increase in pollutant concentration (from 30 to 80 ppm), the total flux (from 153.56 to 58.74 L/m^2.h), and the final net water flux (from 227.72 to 127.74 L/m^2.h) has decreased due to the increased membrane surface fouling; although, the amount of initial pure water flow before passing the pollutant with different concentrations was the same due to the similarity of the conditions. According to the results, to continue the research, the concentration of 80 ppm with the permeate flux of 89.39 L/m^2.h and HA removal of 75.59% was chosen as the optimal concentration.

PEG: TA ratio optimization

In order to select the optimal membrane, flux, removal efficiency, water contact angle, membrane properties, porosity and pore size, and antifouling properties were investigated for all modified membranes at 1.5 bar pressure and 80 ppm pollutant concentration. As seen in Fig. 3 a, with

the increase in PEG additives percentage, the membrane's permeability increased due to the hydrophilicity of the membrane surface by PEG hydroxyl bonds, although this trend has not had a significant impact on rejection. On the other hand, with an increase in the percentage of TA nanoparticles, membrane rejection has also increased. However, it did not significantly improve the membrane permeability, which was probably due to the decrease in the number and size of the membrane pores. In other words, increasing the concentration of nanoparticles has decreased the porosity of the membrane and provided a dense layer on the TA coated membrane's surface, leading to higher pollutant removal. Despite this phenomenon, a decrease in the permeate flux of the mentioned membrane has occurred (Li et al. 2019).

All the membranes had relatively high rejection and approximately good permeability. As observed, the M_1 membrane, covered only with PEG additives, had the highest permeability (131.21 L/m^2.h), and the M_2 membrane, which was covered only with TA nanoparticles, had the highest rejection (88.38%). Therefore, the optimal membrane is the membrane that has the least fouling and the highest removal percentage. Among the membranes M_3, M_4, and M_5, which included nanoparticles and additives, the M_3 membrane, although it had a high flux (127.62 L/m^2.h), had a lower rejection (81.49%) than the two. Among M_4 and M_5 membranes, the M_4 membrane had higher permeability (72.43 L/m^2.h) and rejection (86.62%).

Figure 3 b shows J_{w1}, J_{w2}, and J_p values for modified membranes. According to this Figure, the membranes modified by nanoparticles and additives have higher pure water fluxes than the pristine M_0 membrane, due to the increased hydrophilicity of the membranes modified by nanoparticles and additives. As can be seen, the M_1 membrane had the highest pure water flux (1303.65 L/m^2.h). The M_1 membrane was modified by PEG additives, which contained a hydroxyl bond. The membrane's high hydrophilic properties increased in pure water flux in this vein. The M_5 membrane, which included PEG additives and TA nanoparticles, had a high hydrophilic effect (735.24 L/m^2.h) compared to other membranes. The relatively low flux of the pristine membrane was due to its superhydrophobic property; these results were also

Fig. 3 **a** Separation performance, **b** J_{w1}, J_{w2}, and J_p Flux changes passing through all kinds of membranes during 90 min (P = 1.5 bar, (Nazri et al. 2021) = 80 ppm, pH = 7)
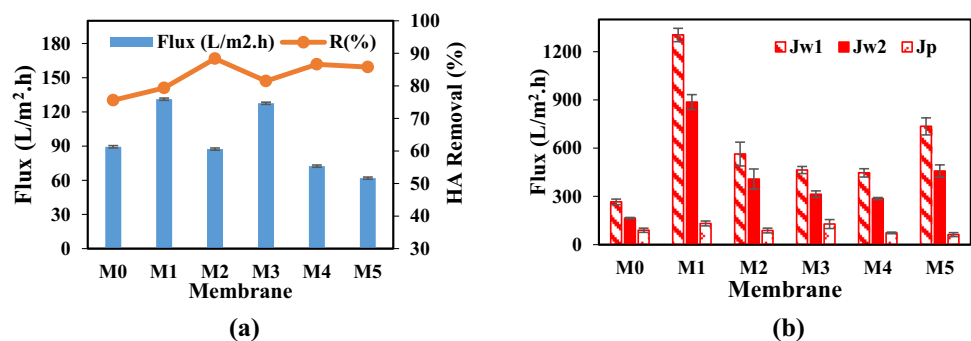
reported in the research of Liu et al. (2021). Furthermore, the flux drop in the last 15 min (313.69 L/m^2.h) compared to the first 30 min of pure water flux (463.75 L/m^2.h) indicates membrane fouling; indeed, a decrease in the flux drop in the M_3 membrane indicated a lower level of fouling in this membrane in comparison to other membranes.

Water contact angle The water contact angle was measured to determine the hydrophilicity of the membrane surface. According to Fig. 4, the contact angle of the water droplet with the membrane surface decreased by modifying the membrane surface, which can be attributed to the presence of hydrophilic hydroxyl (OH) and carboxyl (COOH) groups present in TA nanoparticles and PEG additives. The hydrophilicity of the membrane also meant a decrease in the membrane surface fouling and an increase in flux (for example, M_3 membrane), indicating the presence of nanoparticles on the membrane surface. On the other hand, the nanoparticles that were equal to or smaller than the membrane pores caused the walls of these pores to close, which led to a decrease in the membrane flux (for example, M_4 membrane). Therefore, by coating the membranes with the nanoparticles and creating a surface layer, although the membrane surface became hydrophilic, no continuous trend
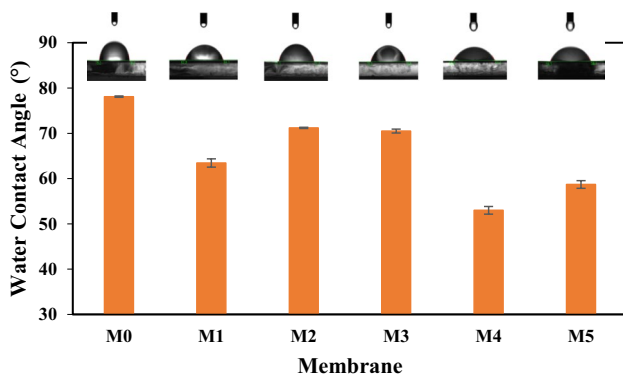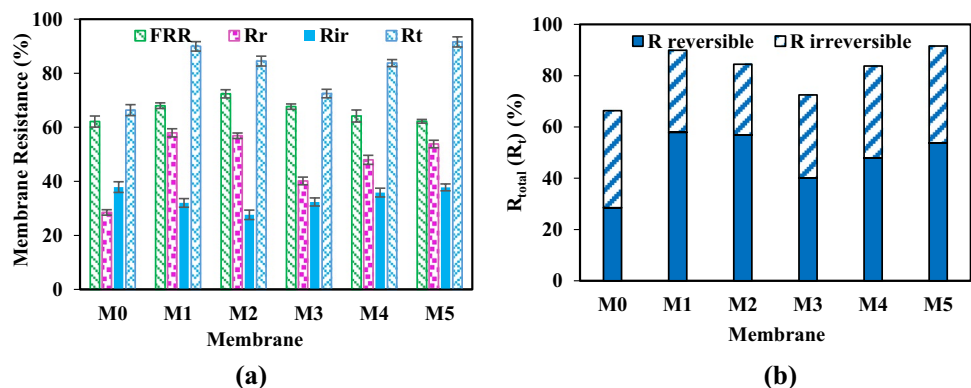

Fig. 4 Contact angle of the mentioned membranes

was observed in the membrane flux. Khezraqa et al. (2022) also reported similar results.

Antifouling characterization The permeability fluxes of HA and pure water were measured to check the antifouling characteristics of the membranes. According to Fig. 5 a, FRR and R_r for all modified membranes were higher than the original pristine membrane, and R_{ir} was the opposite. Figure 5 b also shows the total membrane resistances. The M_2 membrane coated with TA nanoparticles had high hydrophilicity and low water contact angle, which reduced the ability to absorb sediment on the membrane surface; in a way that the presence of water on the surface of the membrane acts like a layer that did not allow the pollutant to enter the membrane pores. Therefore, it had the highest FRR (72.39%). According to Fig. 5 a, b, the increase in R_r by modifying the membranes was due to the reduction of surface hydrophobicity caused by the hydrogen bonding of TA nanoparticles and PEG additives on the membrane polymer surface. In modified membranes, M_1 (57.92%) and M_2 (56.86%) coated with PEG additives and TA nanoparticles, respectively, had higher R_r than other membranes. Also, M_4 (47.93%) and M_5 (53.81%) had more suitable reversible resistances than the M_0 membrane (28.47%). In Kumar et al.'s (2016) studies, an increase in %FRR and R_r in the polysulfone membrane with GO-TiO$_2$ nanoparticles in regard to the separation of HA has been reported. In general, the reduction of R_{ir} and the increase of R_r in the coated membranes compared to the pristine membrane indicates the reusability of the membranes by hydraulic washing (Kallem et al. 2021).

Porosity In order to better compare the membranes and choose the optimal membrane, porosity was also investigated. Membrane porosity is measured according to the number and size of pores in the surface layer of the membrane. An increase in the number and size of holes in the surface layer of the membrane means an increase in porosity and, as a result, an increase in the permeate flux. Coating membranes with nanoparticles and additives improve

Fig. 5 a Membrane resistances, **b** total membrane resistance during 90 min ($P = 1.5$ bar, (Nazri et al. 2021) = 80 ppm, pH = 7)

Table 2 Characterization, permeate flux, removal, and resistance of the considered membranes

Membrane	PEG:TA	J_p (L/m^2.h)	R (%)	FRR (%)	R_r (%)	R_{ir} (%)	R_t (%)	ε (%)	D_m (nm)
M_0	0:0	99.39	75.59	62.12	28.47	37.87	66.34	56.98	21.59
M_1	1:0	131.21	79.37	67.98	57.92	32.01	89.93	73.46	44.59
M_2	0:1	87.4	88.38	72.39	56.86	27.6	84.47	49.38	40.92
M_3	1:1	127.62	81.49	67.64	40.12	32.35	72.48	65.74	29.89
M_4	4:1	72.43	86.62	64.17	47.93	35.82	83.76	46.62	34.24
M_5	1:4	61.9	85.79	62.23	53.81	37.76	91.58	37.03	48.48

their hydrophilicity, which also positively improves porosity. According to Table 2, the modified membranes M_2 (49.38%), M_4 (46.62%) and M_5 (37.03%) had lower porosity than the M_0 pristine membrane (56.98%). Membrane M_1 (73.46%), covered merely with additives, had the highest porosity, which was the justification for the high flux of this membrane. M_3 membrane (65.74%), which had an equal ratio of nanoparticles and additives, also had high porosity. Similar results have been presented in the studies of Kumar et al. (2016); Krishnan et al. (2022). Further, by coating nanoparticles on the membrane surface, the average diameter of the pores increases, which is due to the improvement of hydrophilic properties of membranes by coating nanoparticles. As can be seen in Table 2, M5 (48.48 nm) and M_1 (44.59 nm) had the highest average diameter, followed by M_2 (40.92 nm), M_4 (34.24 nm), and M_3 (29.89 nm). Needless to say, they all had higher average diameters than M_0 (21.59 nm) (Sakarkar et al. 2020).

According to the experiments conducted in this research, a significant increase in pure water permeability flux (446.03 L/m^2.h), membrane rejection (86.62%), and recovery ratio (64.17%) the M_4 membrane compared to pure water permeability flux (265.64 L/m^2.h), membrane rejection (75.59%) and recovery ratio (62.12%) of the M_0 membrane. Furthermore, an increase in reversible resistance (47.93%) and a decrease in irreversible resistance (35.82%) were observed in the M_4 membrane compared to reversible (28.47%), and irreversible resistance (37.87%) of the primary membrane have been observed. On the other hand, with the coating of TA nanoparticles on the membrane surface, the membrane pores were closed with a coating of nanoparticles, which reduced the porosity in the M_4 membrane (46.62%) and also the effluent flux (72.43 L/m^2.h) compared to the porosity (56.98%) and the effluent flux (89.39 L/m^2.h) of M_0 membrane, and the average particle diameter in M_4 membrane (34.24 nm) after M_5 and M_1 membranes, is more favorable than M_0 membrane (21.59 nm). With these in mind, the M_4 membrane was finally chosen as the optimal membrane for further research.

pH optimization

Finally, the effect of pH on the flux and HA removal efficiency of the selected membrane M_4 was investigated (Fig. 6a–c). According to Fig. 6 a, b, with the increase in pH from 5–9, the flux decreased from 167.96 to 27.08 L/m^2.h and the increase in membrane rejection from 80.79 to 96.26% was observed. It was justified according to dynamic light diffraction analysis (Fig. 6 c). Dynamic light diffraction analysis was performed to measure HA zeta potential and its particle size to determine the chemical properties and surface charge created on the membrane surface at pH 5, 7, and 9. In fact, with the increase in pH from 5 to 9, the decrease in the HA zeta potential (at pH 5, 7, and 9, − 14.56 mV, − 21.93 mV, and − 23.86 mV, respectively) and the increase in HA particle size (at pH 5, 7, and 9, respectively, 126.3 nm, 142.1 nm, and 160.3 nm) were observed, in a way that the more acidic the condition, the steeper the slope, and with the increase in pH, the slope decreased to the point where an almost flat line was observed in the alkaline condition. With the increase in the size of the HA particles and the HA zeta potential becoming more negative, it can be concluded that at low pH, the solution has little stability and settles in a viscous and bulky form in the solution. In fact, the functional groups of carboxyl (–COOH) and hydroxyl of HA are protonated, which causes a decrease in density, a decrease in electrostatic repulsion, shrinking of the polymer, and a decrease in the size of the HA particles, which leads to an increase in the average pore size and ultimately an increase in permeability. At high pH, the opposite of this situation occurs; that is, the carboxyl groups are separated into carboxyl ions (–COO$^-$), which causes electrostatic repulsion, increase in density, enlargement of polymer, increase in HA particle size, and as a result, decrease in HA average pore size and ultimately decrease in permeability. In other words, pH has an influential role in HA particle size and membrane surface charge according to the type of membrane and pollutant. In the studies of Mondal et al. (2019), the water flux has decreased in pH 3 to 12 for the glucose pollutant.

Fig. 6 **a** Flux-time, **b** Flux & HA removal (%)-pH c) HA particle size and zeta potential-pH M_4 membrane during 60 min ($P = 1.5$ bar, (Nazri et al. 2021) = 80 ppm)

(a)

(b)

(c)
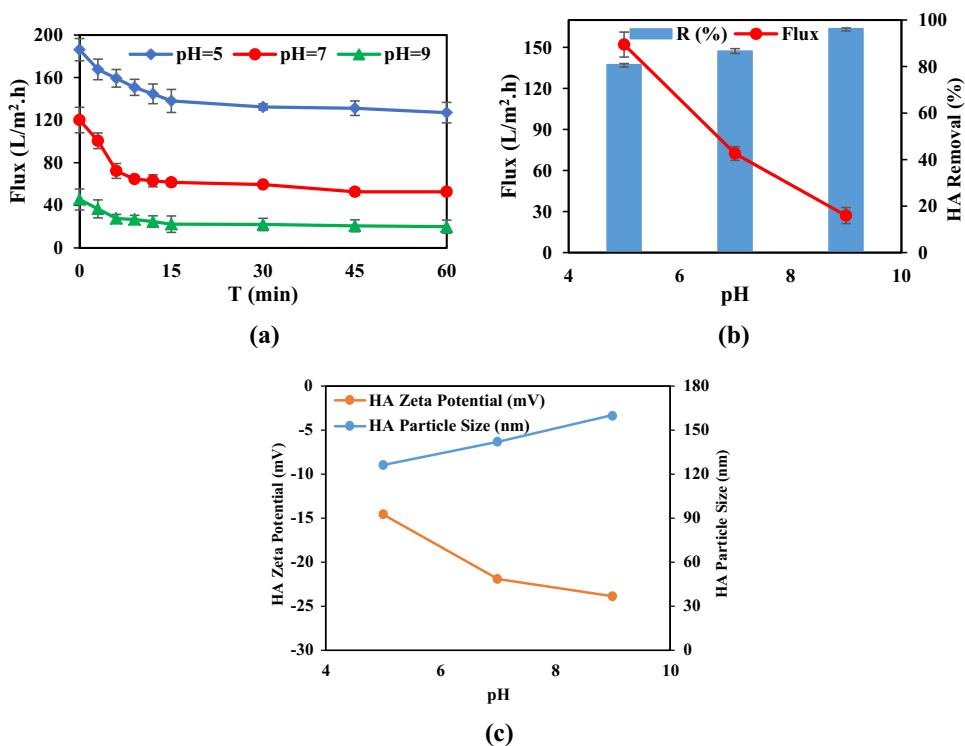
Fig. 7 **a** General flux, **b** J_{w1}, J_{w2}, and J_p Flux changes passing through the M_4 membrane at Different pH of HA during 60 min ($P = 1.5$ bar, (Nazri et al. 2021) = 80 ppm)
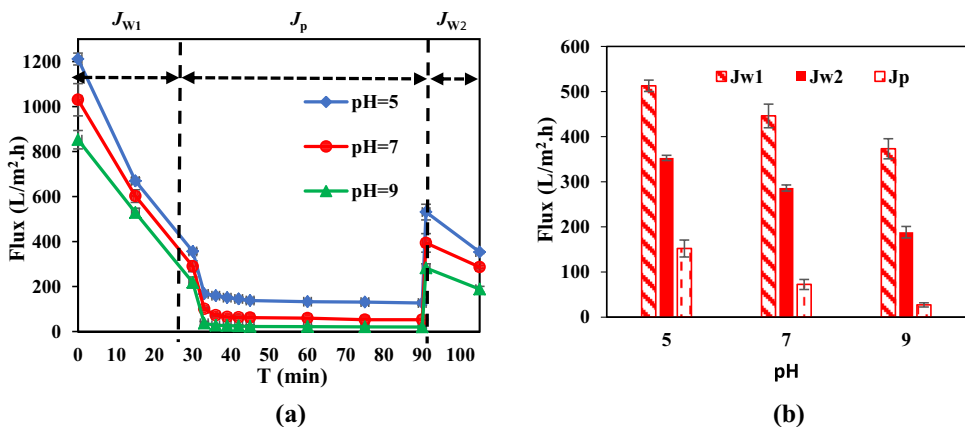

(a)

(b)

Figure 7 a, b, respectively, shows the total permeate flux through the membrane in terms of time and the values of J_{w1}, J_{w2}, and J_p permeating the optimal membrane M_4 at different pHs. According to these two Figures and according to what was said in the previous part, it can be seen that with the increase in pH, the flux through the membrane, including the initial and the final pure water flux, has decreased. According to the results, pH = 5 had the highest total flux (167.96 L/m^2.h), the initial pure water flux (512.70 L/m^2.h), and the lowest amount of HA removal (80.79%) and vice versa pH = 9 had the lowest total flux (27.08 L/m^2.h) and initial pure water flux (373.24 L/m^2.h), and the highest amount of HA removal (96.26%). Thus,

pH = 7, which had a favorable total flux (72.43 L/m^2.h), initial pure water flux (446.03 L/m^2.h), and HA removal rate (86.62%), was selected as pH Optimum.

Membrane characterization

The membranes underwent characterization through analysis. In this regard, ATR-FTIR, FESEM, AFM, and EDS analyses were conducted to comprehensively examine the surface structure and chemical bonding, surface morphology, topography, and elemental composition of membrane surfaces.

**Fig. 8** ATR-FTIR spectra of all five membranes
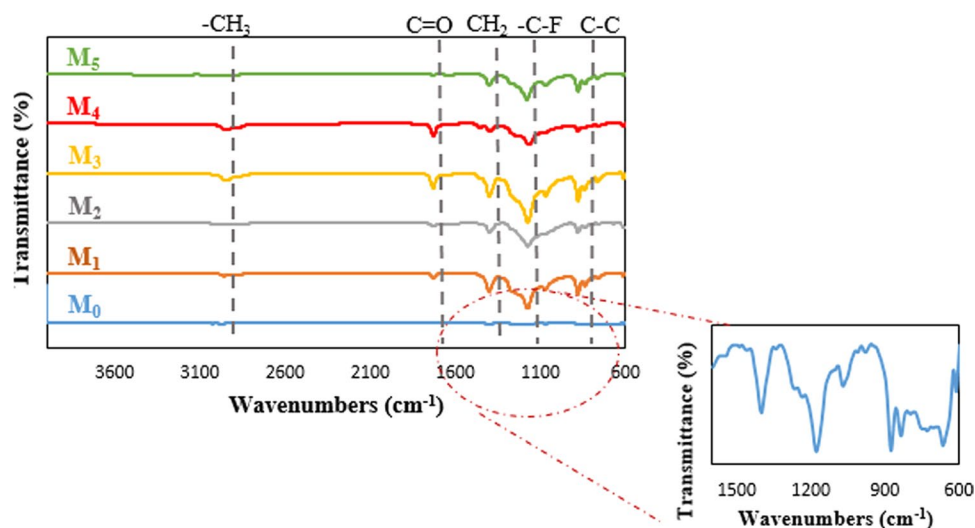
ATR-FTIR analysis

ATR-FTIR spectrum was used to examine the structure and chemical bonding of the surface of all membranes. Figure 8 shows the spectra of all membranes. Compared to the prime pristine membrane, the M_4 membrane had an absorption peak at 1729.81 cm^{-1} due to the stretching vibration of C=O related to the hydrophilic carboxyl group (COOH) present in TA, indicates the proper coverage of TA nanoparticles on the membrane surface. These numbers were observed in the other four modified membranes with a slight change caused by the effect of coated nanoparticles and additives on the membrane surface with different percentages. Based on all the spectra of the modified membranes, it can be concluded that TA nanoparticles and PEG additives are uniformly dispersed on the PVDF membrane, which has also indicated similar results in the studies of Shi et al. (2018) and Turk et al. (2021).

FESEM and AFM analysis

Surface morphology and topography were investigated by FESEM and AFM analysis of the pristine membrane (M_0) and the selected modified membrane (M_4), respectively. As can be seen in the cross-sectional images in Fig. 9 a, the M_0 membrane (PEG: TA = 0:0) has a smooth and uniform surface, indicating the polymer membrane's uniformity and homogeneity. The number of pores in this membrane is less but bigger. The cross-sectional images of the M_0 membrane show high membrane density. In the modified M_4 membrane (PEG: TA = 4:1), the number of pores has increased, but their size has become smaller, which ensures the coating of nanoparticles and additives on the surface of the membrane. Due to the hydrogen bond created between TA nanoparticles and PEG additives in the initial casting solution, masses

have been made, which made the distribution of pores on the surface of the coated membrane not homogeneous. According to the FESEM images shown in Fig. 9 b, in the cross-sectional images of the membrane, two porous and dense spongy parts can be seen, the porous part has asymmetric finger-shaped pores, and the spongy part determines the permeability rate (Jiang et al. 2021; Yang et al. 2020). The M_4 membrane has more regular pores and spongy parts, more porosity, and larger finger pores compared to the M_0 membrane. In fact, with the increase in the percentage of nanoparticles and the hydrophilicity of the polymer matrix, the number of coarse pores decreased, and the finger-shaped holes became more regular in the M_4 membrane. The formation of more pores in the finger-shaped part and fewer in the spongy part of the membrane indicates an increase in hydrophilicity and, consequently, membrane flux. Similar results have been presented in the studies of Li et al. (2019).

Surface roughness is effective on membrane permeability, fouling, and, ultimately, rejection. Therefore, AFM analysis was performed for the M_0 membrane, which was the pristine membrane, and the M_4 membrane, which was more suitable in terms of membrane properties, hydrophilicity, and surface morphology than other modified membranes. As can be seen in Fig. 9 c, with the coating of the membrane surface in the M_4 membrane, R_a increased from 30.98 to 37.10, which can be attributed to the porosity improvement. The highest points of the membrane surface are lighter than depressions and pores. The higher the coefficient of the membrane surface area means the creation of more bumps and depressions on the surface and, indeed, a higher surface roughness. Root mean square roughness can have very different results depending on the occurrence and distribution of surface roughness. The higher the R_q, the more uniform the surface roughness, which in the modified M_4 membrane had a value of 48.83, which indicated the proper distribution
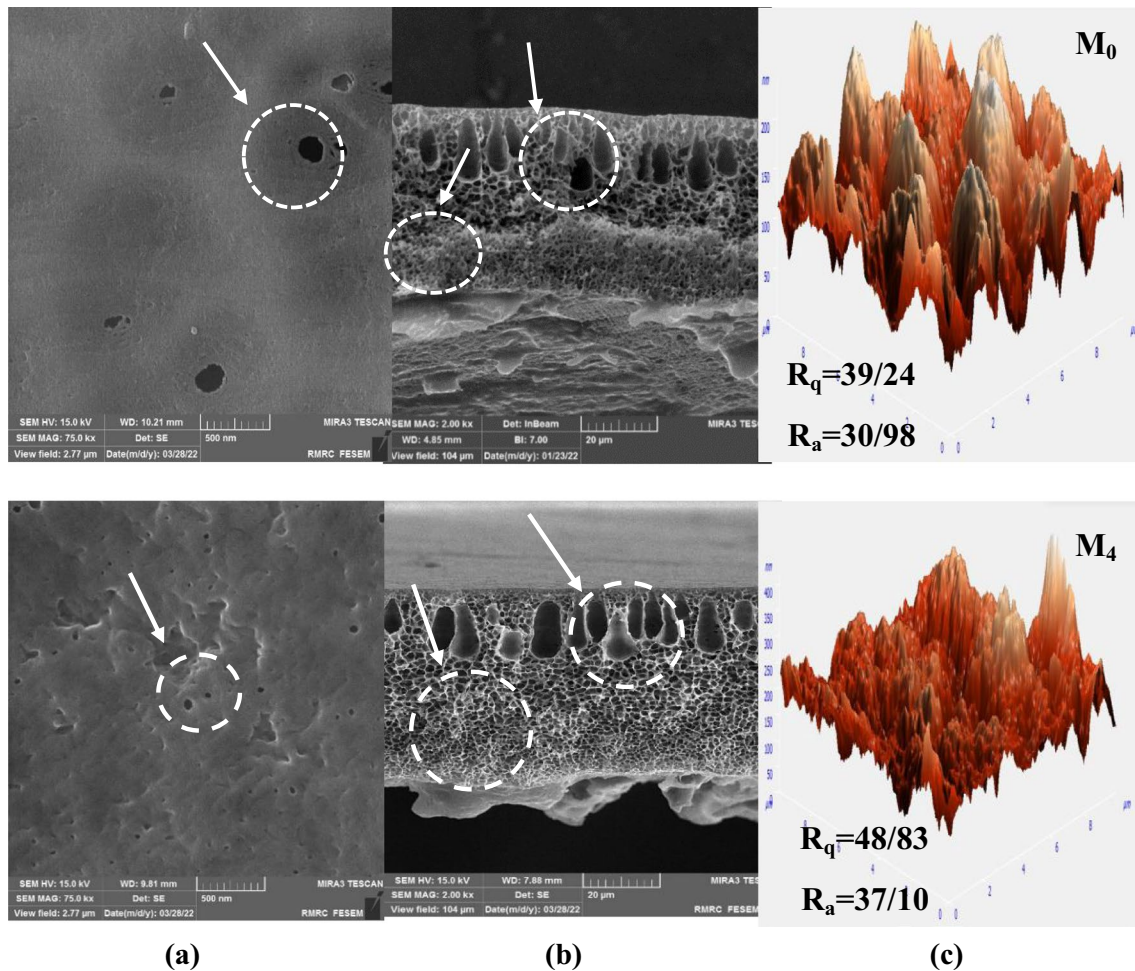
Fig. 9 Images of the M_0 and M_4 membranes **a** FESEM top surface (500 nm), **b** FESEM cross Sect. (20 μm), and **c** AFM (10 μm × 10 μm)

of TA nanoparticles on the membrane surface and was also higher than the M_0 membrane (39.24). In fact, it can be concluded that the membrane polymer solution creates a denser structure and a softer surface. By increasing the amount of nanocomposite and simultaneously with its migration to the membrane surface, the anionic interactions related to the polymer strands cause wrinkles in the modified membrane; accordingly, the roughness of the membrane surface increases (Zhang et al. 2021).

EDS analysis

According to Fig. 10 a, the elemental composition of M_0 and M_4 membrane surfaces was determined by EDS. As can be seen, by covering the surface of the membrane, the amount of carbon elements (from 51.27 to 75.14), oxygen (from 1.05 to 16.11), and nitrogen (from 0.81 to 1.05) in the modified M_4 membrane compared to the pristine M_0 membrane has increased, and the amount of fluorine (from 46.86 to 7.7) has decreased, which is due to the hydroxyl and ether functional

groups present in TA nanoparticles and PEG additives. Similar results have been reported in the studies of Fahrina et al. (2022). These results are also observed in the EDS mapping images, according to Fig. 10 b, the nanoparticles and additives are uniformly and homogeneously dispersed on the M_4 membrane surface. In fact, the fluorine element in the M_0 membrane was high due to the PVDF polymer in the pristine membrane. Additionally, the increase in the carbon element in the modified membrane (M_4) compared to the M_0 membrane was due to the coating of the membrane with TA nanoparticles and PEG additives.
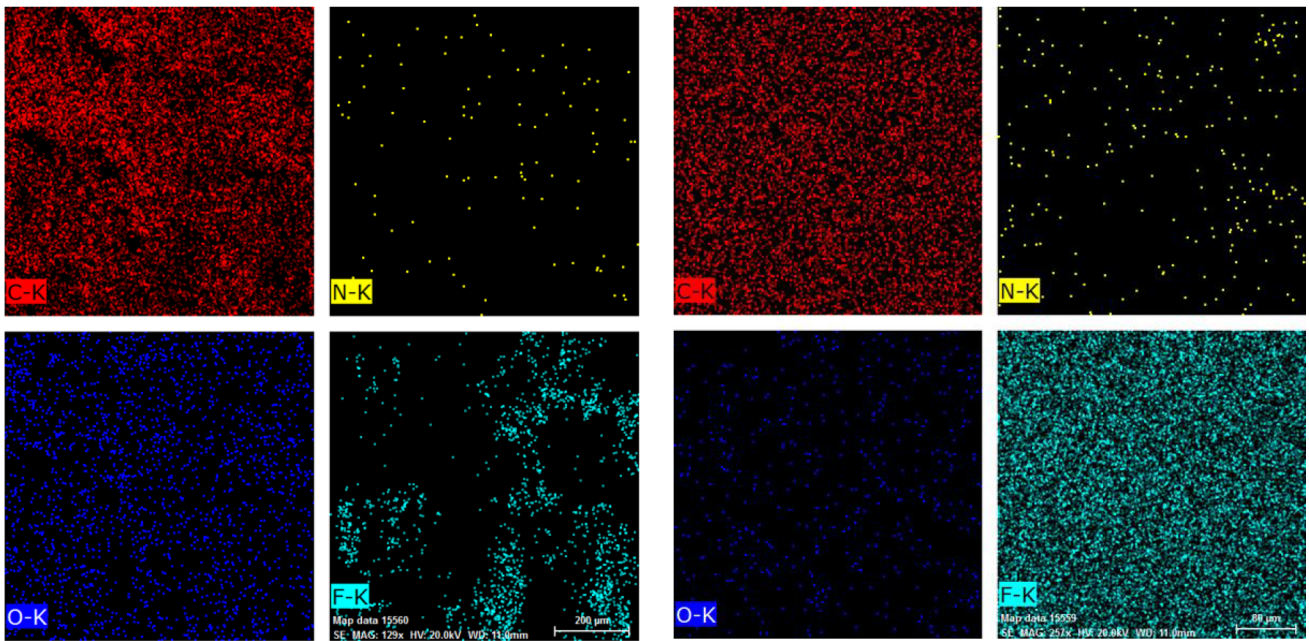
Conclusion

In order to achieve optimal removal efficiency, the PVDF pristine membrane was surface modified with TA nanoparticles and PEG additives in this investigation. Compared to the unmodified pristine membrane, an improvement in pollutant absorption was observed in the membrane modified with TA
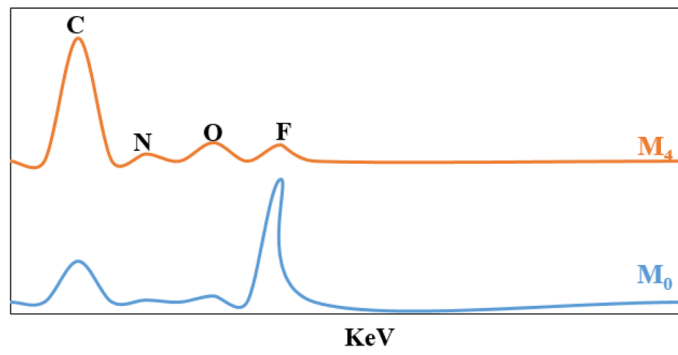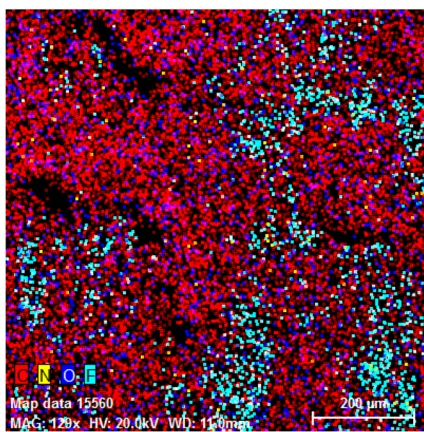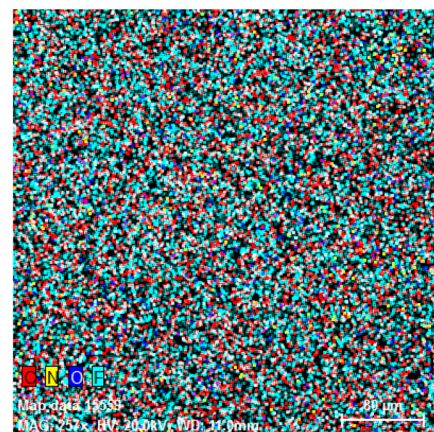
(a)

b.2

b.1

b.4

b.3

Fig. 10 **a** EDS spectra **b** EDX mappings of the membrane surface of (1) M_0, and (2) M_4 membranes and total mappings of (3) M_0 and (4) M_4 membranes

nanoparticles. In fact, the interaction between the –OH in TA nanoparticles and the –O– in PEG additives resulted in the formation of hydrogen bonds, enhancing the membrane's antifouling properties, hydrophilicity, pure water permeate flux, and the pollutant removal efficiency. Still, an increase in the percentage of nanoparticles did not mean an increase in pollutant absorption. Further, the modified membranes did not always exhibit an increase in permeability due to membrane fouling caused by the adsorption of HA particles on the membrane surface. The results showed that by increasing the pressure, the weight percentage of PEG additives, and decreasing the weight percentage of TA nanoparticles, permeability increased and rejection decreased. Also, with the increase of the pollutant concentration, permeability and rejection both decreased. Furthermore, at alkaline pHs, a decrease in permeability and an increase in rejection were observed. According to the analyses performed for different membrane types, the M_4 membrane provided the best performance. Reducing the water contact angle with the coating of nanoparticles and additive on the membrane surface due to the increase of hydrophilic hydroxyl (OH) and carboxyl (COOH) groups, as well as the increase and regularization of pores in the finger-shaped part- so that the coarse pores decreased, but the number of pores increased, causing an increase in pure water flux, which can be related to the coating of these pores by TA nanoparticles. According to the results of this research, the membrane coating method, by affecting the morphology and surface properties of the membrane, effectively changes the flux and removal efficiency of the membrane, as well as the antifouling properties of the membrane.

Data availability The authors declare that the data supporting the findings of this study are available within the article.

Declarations

Conflict of interest The authors have no relevant financial or non-financial interests to disclose. The authors declare that they have no known competing financial interests or personal relationships that could have appeared to influence the work reported in this paper.

Consent for publication The authors give their consent for the publication of identifiable details, which can details within the text (material) to be published in the above Journal and Article.

Ethical approval and consent to participate This material is the authors' own original work, which has not been previously published elsewhere.

References

Abdulazeez I, Salhi B, Elsharif AM, Ahmad MS, Baig N, Abdelnaby MM (2023) Hemin-modified multi-walled carbon nanotube-incorporated PVDF membranes: computational and experimental studies on oil-water emulsion separations. Molecules 28(1):391

Algamdi MS, Alsohaimi IH, Lawler J, Ali HM, Aldawsari AM, Hassan HM (2019) Fabrication of graphene oxide incorporated polyethersulfone hybrid ultrafiltration membranes for humic acid removal. Sep Purif Technol 223:17–23

Alpatova A, Meshref M, McPhedran KN, El-Din MG (2015) Composite polyvinylidene fluoride (PVDF) membrane impregnated with Fe_2O_3 nanoparticles and multiwalled carbon nanotubes for catalytic degradation of organic contaminants. J Membr Sci 490:227–235

D'souza AA, Shegokar R (2016) Polyethylene glycol (PEG): a versatile polymer for pharmaceutical applications. Expert Opin Drug Deliv 13(9):1257–1275

Fahrina A et al (2022) Functionalization of PEG-AgNPs hybrid material to alleviate biofouling tendency of polyethersulfone membrane. Polymers 14(9):1908

Fan G et al (2021) Enhancing the antifouling and rejection properties of PVDF membrane by Ag_3PO_4–GO modification. Sci Total Environ 801:149611

He PY, Zhang YJ, Chen H, Han ZC, Liu LC (2020) Low-cost and facile synthesis of geopolymer-zeolite composite membrane for chromium (VI) separation from aqueous solution. J Hazard Mater 392:122359

Jiang B, Cheng K, Zhang N, Yang N, Zhang L, Sun Y (2021) One-step modification of PVDF membrane with tannin-inspired highly hydrophilic and underwater superoleophobic coating for effective oil-in-water emulsion separation. Sep Purif Technol 255:117724

Kallem P, Othman I, Ouda M, Hasan SW, AlNashef I, Banat F (2021) Polyethersulfone hybrid ultrafiltration membranes fabricated with polydopamine modified $ZnFe_2O_4$ nanocomposites: applications in

humic acid removal and oil/water emulsion separation. Process Saf Environ Prot 148:813–824

Karimi A, Khataee A, Ghadimi A, Vatanpour V (2021) Ball-milled Cu_2S nanoparticles as an efficient additive for modification of the PVDF ultrafiltration membranes: application to separation of protein and dyes. J Environ Chem Eng 9(2):105115

Khezraqa H, Etemadi H, Qazvini H, Salami-Kalajahi M (2022) Novel polycarbonate membrane embedded with multi-walled carbon nanotube for water treatment: a comparative study between bovine serum albumin and humic acid removal. Polym Bull 79(3):1467–1484

Khoo YS, Lau WJ, Liang YY, Karaman M, Gürsoy M, Ismail AF (2022) Eco-friendly surface modification approach to develop thin film nanocomposite membrane with improved desalination and antifouling properties. J Adv Res 36:39–49

Krishnan SG, Abinaya S, Arthanareeswaran G, Govindaraju S, Yun K (2022) Surface-constructing of visible-light Bi_2WO_6/CeO_2 nanophotocatalyst grafted PVDF membrane for degradation of tetracycline and humic acid. J Hazard Mater 421:126747

Kumar M, Gholamvand Z, Morrissey A, Nolan K, Ulbricht M, Lawler J (2016) Preparation and characterization of low fouling novel hybrid ultrafiltration membranes based on the blends of $GO–TiO_2$ nanocomposite and polysulfone for humic acid removal. J Membr Sci 506:38–49

Kusworo TD, Ariyanti N, Utomo DP (2020) Effect of nano-TiO_2 loading in polysulfone membranes on the removal of pollutant following natural-rubber wastewater treatment. J Water Process Eng 35:101190

Li M, Wu L, Zhang C, Chen W, Liu C (2019) Hydrophilic and antifouling modification of PVDF membranes by one-step assembly of tannic acid and polyvinylpyrrolidone. Appl Surf Sci 483:967–978

Li C et al (2020) High-performance electrocatalytic microfiltration CuO/carbon membrane by facile dynamic electrodeposition for small-sized organic pollutants removal. J Membr Sci 601:117913

Liu S et al (2021) Multi-functional tannic acid (TA)-ferric complex coating for forward osmosis membrane with enhanced micropollutant removal and antifouling property. J Membr Sci 626:119171

Luo J, Chen W, Song H, Liu J (2020) Antifouling behaviour of a photocatalytic modified membrane in a moving bed bioreactor for wastewater treatment. J Clean Prod 256:120381

Makhetha T, Moutloali R (2018) Antifouling properties of Cu (tpa)@GO/PES composite membranes and selective dye rejection. J Membr Sci 554:195–210

Mat Nawi NI et al (2020) Development of hydrophilic PVDF membrane using vapour induced phase separation method for produced water treatment. Membranes 10(6):121

Mohd Yatim NS, Boon Seng O (2019) Fluorosilaned-TiO_2/PVDF membrane distillation with improved wetting resistance for water recovery from high solid loading wastewater. J Membr Sci Res 5(1):55–64

Mondal P, Samanta NS, Meghnani V, Purkait MK (2019) Selective glucose permeability in presence of various salts through tunable pore size of pH responsive PVDF-co-HFP membrane. Sep Purif Technol 221:249–260

Nazri AI, Ahmad AL, Hussin MH (2021) Microcrystalline cellulose-blended polyethersulfone membranes for enhanced water permeability and humic acid removal. Membranes 11(9):660

Ni C, Zheng X, Zhang Y, Zhang X, Li Y (2021) Multifunctional porous materials with simultaneous high water flux, antifouling and antibacterial performances from ionic liquid grafted polyethersulfone. Polymer 212:123183

Oulad F, Zinadini S, Zinatizadeh AA, Derakhshan AA (2020) Fabrication and characterization of a novel tannic acid coated boehmite/

PES high performance antifouling NF membrane and application for licorice dye removal. Chem Eng J 397:125105

Ren J, Xia W, Feng X, Zhao Y (2022) Surface modification of PVDF membrane by sulfonated chitosan for enhanced anti-fouling property via PDA coating layer. Mater Lett 307:130981

Sakarkar S, Muthukumaran S, Jegatheesan V (2020) Evaluation of polyvinyl alcohol (PVA) loading in the PVA/titanium dioxide (TiO_2) thin film coating on polyvinylidene fluoride (PVDF) membrane for the removal of textile dyes. Chemosphere 257:127144

Shi P, Hu X, Wang Y, Duan M, Fang S, Chen W (2018) A PEG-tannic acid decorated microfiltration membrane for the fast removal of rhodamine B from water. Sep Purif Technol 207:443–450

Singh R, Purkait MK (2016) Evaluation of mPEG effect on the hydrophilicity and antifouling nature of the PVDF-co-HFP flat sheet polymeric membranes for humic acid removal. J Water Process Eng 14:9–18

Sl T, Äœnlü B, Mustapa MS (2021) Preparation of innovative PEG/tannic acid/TiO_2 hydrogels and effect of tannic acid concentration on their hydrophilicity. Int J Integr Eng 13(7):266–273

Sun F et al (2021) Dopamine-decorated lotus leaf-like PVDF/TiO_2 membrane with underwater superoleophobic for highly efficient oil-water separation. Process Saf Environ Prot 147:788–797

Tajik M, Lashkarbolooki M, Peyravi M (2023) Mechanistic fouling study of hybrid imidazolium-based ionic liquid membrane during emulsified oil removal from oily wastewater; oil type effect. J Environ Chem Eng 11(5):111096

Tajik M, Peyravi M, Lashkarbolooki M (2024) Modified PES membrane by imidazolium-based ionic liquid to investigate fouling by oily foulant: theoretical and experimental study. J Water Process Eng 60:105086

Teow Y, Ooi B, Ahmad A (2017) Study on PVDF-TiO_2 mixed-matrix membrane behaviour towards humic acid adsorption. J Water Process Eng 15:99–106

Teow YH, Ooi BS, Ahmad AL, Lim JK (2020) Investigation of antifouling and UV-cleaning properties of PVDF/TiO_2 mixed-matrix membrane for humic acid removal. Membranes 11(1):16

Xu L et al (2018) A comprehensive description of the threshold flux during oil/water emulsion filtration to identify sustainable flux regimes for tannic acid (TA) dip-coated poly (vinylidene fluoride) (PVDF) membranes. J Membr Sci 563:43–53

Xu S et al (2020) Polyphenol engineered membranes with dually charged sandwich structure for low-pressure molecular separation. J Membr Sci 601:117885

Yan L et al (2022) Bio-inspired mineral-hydrogel hybrid coating on hydrophobic PVDF membrane boosting oil/water emulsion separation. Sep Purif Technol 285:120383

Yang J, Wang L, Xie A, Dai X, Yan Y, Dai J (2020) Facile surface coating of metal-tannin complex onto PVDF membrane with underwater superoleophobicity for oil-water emulsion separation. Surf Coat Technol 389:125630

Yong M, Zhang Y, Sun S, Liu W (2019) Properties of polyvinyl chloride (PVC) ultrafiltration membrane improved by lignin: hydrophilicity and antifouling. J Membr Sci 575:50–59

Zhang N, Song X, Chen Y, Jiang B, Zhang L, Jiang H (2021) A facile and economic route assisted by trace tannic acid to construct a high-performance thin film composite NF membrane for desalination. Environ Sci: Water Res Technol 7(5):956–968

Zhao J, Yang Y, Li C, Hou L-A (2019) Fabrication of GO modified PVDF membrane for dissolved organic matter removal: removal mechanism and antifouling property. Sep Purif Technol 209:482–490